

# Tuning hyperparameters of doublet-detection methods for single-cell RNA sequencing data

Nan Miles Xi <sup>a,\*</sup> and Angelos Vasilopoulos <sup>a</sup>

<sup>a</sup> *Department of Mathematics and Statistics, Loyola University Chicago, Chicago, IL 60660, USA*

\* Correspondence: Nan Miles Xi ([mxil@luc.edu](mailto:mxil@luc.edu))

## Abstract

The existence of doublets in single-cell RNA sequencing (scRNA-seq) data poses a great challenge in downstream data analysis. Computational doublet-detection methods have been developed to remove doublets from scRNA-seq data. Yet, the default hyperparameter settings of those methods may not provide optimal performance. Here, we propose a strategy to tune hyperparameters for a cutting-edge doublet-detection method. We utilize a full factorial design to explore the relationship between hyperparameters and detection accuracy on 16 real scRNA-seq datasets. The optimal hyperparameters are obtained by a response surface model and convex optimization. We show that the optimal hyperparameters provide top performance across scRNA-seq datasets under various biological conditions. Our tuning strategy can be applied to other computational doublet-detection methods. It also offers insights into hyperparameter tuning for broader computational methods in scRNA-seq data analysis.

**Keywords:** scRNA-seq; doublet detection; hyperparameter tuning; experimental design; response surface model

## Introduction

Single-cell RNA sequencing (scRNA-seq) is a cutting-edge sequencing technology that can quantify genome-wide gene expression levels in a large number of cells <sup>1,2</sup>. Since its debut, scRNA-seq has been widely applied in various fields, including precision medicine <sup>3</sup>, drug discovery <sup>4</sup>, cancer therapy <sup>5</sup>, and vaccine development <sup>6</sup>. The successful application of scRNA-seq relies on separating and labeling mRNA molecules from different cells. However, results may be confounded by the formation of doublets — when two cells are captured in one reaction volume by chance <sup>7</sup>. Because doublets appear as but are not real cells, they potentially bias downstream scRNA-seq data analysis. For example, doublets may be falsely identified as new cell types in cell clustering analysis <sup>8</sup>. To tackle this issue, the scRNA-seq community has developed computational methods to detect doublets from scRNA-seq data <sup>7–11</sup>. These methods utilize statistical and machine learning models, each with a set of default hyperparameters. Despite rapid development in methodology, one critical question remains untouched: whether default hyperparameters offer the best doublet-detection performance, especially for scRNA-seq datasets generated under various biological conditions.

Here, we systematically explore the optimal hyperparameters of scDblFinder <sup>9</sup>, one cutting-edge computational doublet-detection method. We collect detection accuracy data for various hyperparameter combinations from 16 real scRNA-seq datasets with experimentally annotated doublets. Then, we fit a second-degree polynomial regression model with first-order, second-order, and interaction terms of three key hyperparameters. Convex optimization is performed to find the hyperparameters that maximize average detection accuracy across 16 datasets. We show that our optimal hyperparameters significantly improve doublet-detection accuracy over the method's default settings on most datasets. The detection accuracy of our optimal hyperparameters also ranks close to the best performance obtained by exhaustive searches in many datasets. We also apply our tuning strategy to scRNA-seq datasets under various biological conditions using different double-detection measurements. We find similar benefits from hyperparameter tuning, and the optimal hyperparameters vary depending on the biological conditions and accuracy measurements. Our exploratory strategy can be easily extended to other computational doublet-detection methods and provides hyperparameter tuning insights for broader computational methods in scRNA-seq data analysis.

## Datasets

In this study, we utilize 16 public scRNA-seq datasets collected in a previous benchmark study<sup>12</sup>. All datasets contain ground-truth doublet labels annotated by experimental techniques. They are so far the most comprehensive scRNA-seq data collection with ground-truth doublet labels. The datasets cover a wide range of cell types, droplet numbers, gene numbers, and doublet rates, representing various difficulty levels in detecting doublets from scRNA-seq data. [Table 1](#) summarizes the key characteristics of the 16 datasets used in this study. In scRNA-seq experiments, droplets refer to the reaction volumes that encapsulate the cell suspension. While most droplets contain one cell (singlets) as expected, others accidentally encapsulate two cells (doublets). Therefore, we will use “droplet” instead of “cell” to denote one data point in scRNA-seq datasets in the following text.

## Hyperparameter setting

We choose scDbfFinder as the target method for exploring optimal hyperparameter settings. The design of scDbfFinder can be summarized in the following steps. First, it generates artificial doublets by combining gene expression profiles of two randomly selected droplets in the dataset. Second, it conducts PCA dimension reduction on the union of artificial doublets and true droplets using top highly variable genes. Third, scDbfFinder constructs a nearest neighbor network on top of the low-dimensional representations from the dimension reduction. Fourth, it sets different neighborhood sizes to create multiple predictors that will be used for binary classification. Finally, it performs cross-validation to assign a doublet score to each droplet. In each iteration of cross-validation, it trains a gradient boosting model to distinguish true droplets and artificial doublets in the training set, and then assigns each droplet in the test set a doublet probability (doublet score). The design of scDbfFinder helps to reduce the impact of batch effects on doublet detection: since cross-validation randomly assigns droplets from different batches to training and test sets, the batch effects will not cause the domain shift problem<sup>13</sup> in the final classification step.

scDbfFinder has shown superior performance in previous benchmark studies<sup>12,14</sup>. We consider three key hyperparameters of scDbfFinder, i.e., the number of top features, the number of top principal components, and the maximum depths of decision trees. We refer to them as  $nf$ ,  $pc$ , and

*depth* moving forward, respectively. These three hyperparameters are discrete numerical variables, and we set each of them to five different levels (Table 2). Therefore, there are  $5 \times 5 \times 5 = 125$  hyperparameter combinations in total. In experimental design literature, this is a  $3^5$  full factorial design<sup>15</sup>. It allows investigation of the effects of individual hyperparameters, as well as the effects of interactions between different hyperparameters on the performance of doublet detection.

We choose the five values for each hyperparameter according to the following rule. First, we start with the default values of each hyperparameter (Table 2). In general, the default values are selected by the developers based on extensive numerical experiments and thus are likely close to a local optimum in the hyperparameter space. Second, with the default value as the center, we increase or decrease each hyperparameter by one or several fixed step sizes, generating four extra alternative values. We determine the step size and the search space boundaries for each hyperparameter based on the common practice in scRNA-seq data analysis.

The hyperparameter *nf* refers to the number of highly variable genes used in the downstream analysis. Its value is often set from several hundred to several thousand in many applications. For example, scDblFinder uses 1000 as the default value and Seurat<sup>16</sup>, a popular R package for scRNA-seq data analysis, chooses 2000. After including these two values in our search space, we insert 1500, the median value between 1000 and 2000, as the third search value, resulting in a step size of 500. We further expand the search space downward and upward by one step size separately. The final search space for *nf* is 500, 1000, 1500, 2000, and 2500.

The hyperparameter *pc* is the number of principal components used in the downstream analysis after performing PCA dimension reduction on highly variable genes. Its value is often set from single digits to several dozen in practice. For example, the Seurat tutorial suggests exploring between 5 to 20 for various scenarios. We start with the default value of 10 and include 5 (the lower bound suggested by Seurat) in the search space, using a step size of 5. We further expand the search space by three step sizes up to 25. The final search space for *pc* is 5, 10, 15, 20, and 25.

The hyperparameter *depth* is the maximum depth of decision trees in the gradient boosting model used in scDblFinder. The larger values indicate more complex gradient boosting models in binary classification (singlet vs. doublet). This hyperparameter is often set to below ten in ordinary

classification tasks to avoid overfitting. For example, XGBoost <sup>17</sup>, a generic gradient boosting package, chooses 6 as the default value. We use scDbfFinder’s default value of 4 as the center of the search space. With 6 as the maximum and 1 as the step size, we create a final search space for *depth* including 2, 3, 4, 5, and 6.

## Doublet detection

We use the R package DoubletCollection <sup>14</sup> to execute scDbfFinder on 16 real datasets with the 125 hyperparameter combinations listed in Table 2. Since doublet detection is essentially a binary classification task, we use the area under the precision-recall curve (AUPRC) to measure the overall doublet-detection accuracy. After execution, each dataset results in a  $125 \times 4$  data matrix, in which the first three columns are *nf*, *pc*, and *depth*, and the last column is AUPRC. Each row in the data matrix represents one combination of three hyperparameters and corresponding AUPRC. The 16 scRNA-seq datasets generate 16 such data matrices. Finally, we merge the 16 data matrices by averaging their AUPRCs for each hyperparameter combination. The final data matrix is  $125 \times 4$ , which contains the relationship between hyperparameters and overall doublet-detection accuracy. We refer to this data matrix as detection accuracy data moving forward.

## Model setup and optimization

We build a second-degree polynomial regression model to examine the relationship between hyperparameters and doublet-detection accuracy. Specifically, we set average AUPRC as the response variable and the first order of the three hyperparameters, the second order of the three hyperparameters, and their interactions as the independent variables. Model (1) shows the complete setup of this second-degree polynomial regression.

$$AUPRC = \beta_0 + \beta_1 nf + \beta_2 pc + \beta_3 depth + \beta_4 nf^2 + \beta_5 pc^2 + \beta_6 depth^2 + \beta_7 nfpc + \beta_8 nfdepth + \beta_9 pcdepth + \epsilon \quad (1)$$

where  $\beta_i, i = 0, 1, \dots, 9$ , are the unknown model parameters, and  $\epsilon$  is the random error.

Second-degree polynomial regression is one classic model in the response surface methodology (RSM) <sup>18</sup>. It is commonly used to explore the relationship between several independent variables (hyperparameters) and one response variable (AUPRC) based on a full factorial design <sup>19</sup>. It can obtain an optimal response by estimating hyperparameters' main and quadratic effects and interactions between them. The second-degree polynomial regression balances model complexity and interpretation, while higher-degree models may cause overfitting and are harder to interpret.

We fit this model by least square estimation using detection accuracy data. We perform a  $t$ -test to assess the significance of estimated parameters  $\hat{\beta}_i$  and set 0.01 as the  $p$ -value cutoff. We find that the first and second orders of  $nf$  and  $pc$  are significant. Equation (2) shows the estimated model (1) with significant independent variables (including the intercept).

$$AUPRC = 5.444 \times 10^{-1} + 1.016 \times 10^{-5}nf + 1.336 \times 10^{-3}pc - 3.760 \times 10^{-9}nf^2 - 3.484 \times 10^{-5}pc^2 \quad (2)$$

To obtain the  $nf$  and  $pc$  that maximize AUPRC, we take the partial derivative of AUPRC in respect of  $nf$  and  $pc$  in (2) and let the derivatives equal zero simultaneously.

$$\begin{cases} \frac{\partial AUPRC}{\partial nf} = 1.016 \times 10^{-5} - 7.520 \times 10^{-9}nf = 0 \\ \frac{\partial AUPRC}{\partial pc} = 1.336 \times 10^{-3} - 6.968 \times 10^{-5}pc = 0 \end{cases} \quad (3)$$

Solving (3) gives the optimal  $nf$  and  $pc$  (after rounding to the nearest integers).

$$\begin{cases} nf = 1352 \\ pc = 19 \end{cases} \quad (4)$$

## Model diagnostics

The 16 scRNA-seq datasets are generated by different sequencing protocols using various doublet annotation techniques. The error terms in model (1) may have non-constant variance, causing the heterogeneity issue. We conduct model diagnostics to examine the existence and severity of

heterogeneity. First, we plot the residue against the fitted value of model (1). [Supplementary Figure S1a](#) shows that most residues have constant variance with no obvious patterns. The only concern is on the left, where the six residues may have a smaller variance. Second, we perform a Breusch-Pagan test<sup>20</sup> for heterogeneity. With the  $p$ -value as 0.451, we fail to reject the null hypothesis that constant variance is present.

Additionally, we perform a sensitivity analysis to examine the robustness of model (1). We conduct a natural log transformation and a square root transformation on the response variable AUPRC in the detection accuracy data. We then fit model (1) on the two transformed datasets and obtain the optimal hyperparameters using the same optimization method in (3). We find that the significant hyperparameters in model (1) and their optimal values are identical (after rounding to the nearest integers) to the results without transformation ([Supplementary Table S1](#)). The patterns of residue plots ([Supplementary Figures S1b](#) and [S1c](#)) are also similar to those before transformation ([Supplementary Figure S1a](#)). Log transformation and square root transformation on the response variable are common remedies for heterogeneity. If heterogeneity exists, then these two transformations would significantly change the model fitting, optimization, and residue plot. Similar results before and after transformations indicate that the heterogeneity is very mild, if any. We suspect that the heterogeneity is largely reduced or removed by averaging the AUPRCs of 16 datasets when creating the detection accuracy data (on which we fit model (1)).

## Optimal hyperparameter evaluation

The optimal hyperparameters in equation (4) are obtained by maximizing the *average* AUPRC across 16 scRNA-seq datasets. To examine if these parameters can improve doublet-detection accuracy on individual datasets, we execute scDbIFinder with  $nf$  and  $pc$  as in (4) on all 16 scRNA-seq datasets. Since hyperparameter *depth* is not significant in model (1), we set it to the default value in the execution. [Table 3](#) compares the AUPRCs of the optimal hyperparameters in equation (4), the method's default hyperparameters, and the maximal AUPRCs achieved by one of 125 hyperparameter combinations. Our optimal hyperparameters outperform the method's performance with default settings on 12 out of 16 scRNA-seq datasets. [Figure 1](#) summarizes the AUPRC improvement by hyperparameters tuning over the method's default settings. The most

significant improvement is over 5% on dataset pbmc-1B-dm. There are eight datasets on which the improvement is over 2%. [Figure 2](#) shows each dataset's AUPRC ranking under optimal hyperparameters among 125 hyperparameter combinations. We can see that the AUPRCs of optimal hyperparameters rank at or higher than the 20<sup>th</sup> percentile on ten datasets. The highest ranking is 3<sup>rd</sup> on dataset pdx-MULTI. The optimal hyperparameters also achieve the 50<sup>th</sup> percentile or higher on all 16 datasets.

## Tuning hyperparameters for various biological conditions

The previous analysis presents the optimal hyperparameters based on the average of 16 scRNA-seq datasets. In practice, users mainly conduct doublet detection on datasets generated under specific biological or technical conditions. Those datasets need unique hyperparameter settings to achieve optimal performance. To demonstrate the generability of our tuning strategy to those applications, we replicate the hyperparameter optimization on two subsets of 16 datasets.

The first is the pbmc-related subset, including six datasets: pbmc-1A-dm, pbmc-1B-dm, pbmc-1C-dm, pbmc-2ctrl-dm, pbmc-2stim-dm, and pbmc-ch. We find that the optimal  $pc$  is 18 (after rounding to the nearest integer), with the other two hyperparameters insignificant ([Supplementary Table S2](#)). [Supplementary Table S3](#) compares the AUPRCs of the optimal hyperparameters, the method's default hyperparameters, and the maximal AUPRCs achieved by one of 125 hyperparameter combinations on pbmc-related datasets. [Supplementary Figure S2a](#) shows each dataset's AUPRC improvement by hyperparameters optimization over the method's default settings, and AUPRC ranking under optimal hyperparameters among 125 hyperparameter combinations. Compared with the optimization on all 16 datasets ([Figures 1 and 2](#)), the AUPRC improvement is greater with hyperparameters specifically tuned for pbmc-related datasets.

The second subset includes the three HMEC-related datasets: HMEC-orig-MULTI, HMEC-rep-MULTI, and HEK-HMEC-MULTI. We find that the optimal  $nf$  is 1520 (after rounding to the nearest integer), with the other two hyperparameters insignificant ([Supplementary Table S2](#)). [Supplementary Table S4](#) compares the AUPRCs of the optimal hyperparameters, the method's default hyperparameters, and the maximal AUPRCs achieved by one of 125 hyperparameter combinations on HMEC-related datasets. [Supplementary Figure S2b](#) shows each dataset's



AUPRC improvement by hyperparameters optimization over the method's default settings, and AUPRC ranking under optimal hyperparameters among 125 hyperparameter combinations. Compared with the optimization on all 16 datasets (Figures 1 and 2), the AUPRC improvement is greater with hyperparameters specifically tuned for HMEC-related datasets.

The two analyses provide guidance for choosing appropriate hyperparameters for specific biological conditions. Future studies can easily expand our tuning strategies to other cell types or platforms if datasets with doublet labels under more diverse biological and technical conditions are available. For example, users can optimize hyperparameters for different sequencing protocols (Smart-seq2, Drop-seq, Chromium, et al.) or the combinations of biological and technical conditions (pbmc and Drop-seq, HMEC and Smart-seq2, et al.).

## **Tuning hyperparameters for various measurements**

The previous analyses use AUPRC, an overall accuracy measurement of doublet detection, as the optimization objective. In practice, users may also be interested in the method's capacity to identify doublets or singlets, i.e., the true positive or negative rate. Different from AUPRC, the calculation of true positive/negative rate requires a user-specified doublet rate. The true doublet rate is typically unknown to the users and needs to be estimated based on the sequencing platform, sequencing throughput, and prior knowledge<sup>12,21</sup>. Because optimization relies on the doublet rate, it is infeasible to find universal optimal hyperparameters for the true positive/negative rate.

To provide hyperparameter guidance under this scenario, we set the doublet rates to their true values for each dataset (Table 1) and calculate the corresponding true positive/negative rates for 125 hyperparameter combinations. Then we replicate our tuning strategy using these two measurements as objectives. We find that the optimal maximum depths of decision trees (*depth*) is 5 for both measurements (after rounding to the nearest integer), with the other two hyperparameters insignificant (Supplementary Table S2). Supplementary Figure S3a and Table S5 show each dataset's true positive rate improvement by hyperparameters optimization over the method's default settings and true positive rate ranking under optimal hyperparameters among 125 hyperparameter combinations. Most datasets exhibit similar improvement as AUPRC, except for J293t-dm, with a 29% increase, significantly larger than others. Such a difference indicates this

dataset's unique biological and technical characteristics, which require stronger hyperparameter tuning efforts.

[Supplementary Figure S3b](#) and [Table S6](#) show each dataset's true negative rate improvement and ranking. Although most datasets still benefit from hyperparameter tuning, the improvement of the true negative rate is milder (below 1%) compared to other metrics. One reason is that the true negative rates under default hyperparameters are already high on many datasets (above 0.95, [Supplementary Table S6](#)), limiting the improvement space by hyperparameter optimization. It is worth noting that the optimal hyperparameters and corresponding true positive/negative rates are obtained using the true doublet rates. If users choose different doublet rates, the optimization results will be different. It is straightforward to generalize our tuning strategy in those cases.

## Discussion

The existence of doublets is a key confounder in scRNA-seq data analysis. With the wide application of scRNA-seq technologies, much effort has been invested in developing computational doublet-detection methods. Such methods are primarily based on statistical and machine learning algorithms and are sensitive to hyperparameter configurations<sup>22</sup>. Although most methods provide a set of default hyperparameters, they cannot guarantee the best doublet-detection performance universally, especially when scRNA-seq data are generated under various biological conditions<sup>23,24</sup>.

In this study, we utilize a full factorial design to build a model of hyperparameters and overall doublet-detection accuracy based on a leading method, scDbtFinder, and 16 scRNA-seq datasets. The optimal hyperparameter combination obtained by convex optimization not only surpasses the default setting but also offers close-to-best detection accuracy on many datasets. We expand our optimization strategy to two subgroups of 16 datasets separately, providing optimal parameters for various biological conditions. We show that our method can also be applied to optimize different measurements of doublet-detection accuracy.

The improved doublet-detection performance by hyperparameter tuning presents several insights regarding the data generalization and doublet annotation mechanisms. First, there are two datasets, hm-6k and hm-12k, whose doublets are annotated by species mixture<sup>25</sup>. Both have lower AUPRCs

using optimal hyperparameters than default hyperparameters (Figure 1). In contrast, most datasets generated by the other three doublet annotation techniques, i.e., cell hashing<sup>26</sup>, demuxlet<sup>27</sup>, and MULTI-seq<sup>28</sup>, benefit from hyperparameter tuning. One possible reason is due to their different doublet-annotation mechanisms. While species mixture can only annotate doublets from two species, the other three techniques utilize oligo-tagged antibody, SNP, or lipid-tagged index to label doublets from much broader sources. Consequently, the true doublets in hm-6k and hm-12k are likely undercounted, causing their inconsistent optimization results.

Second, the hyperparameter tuning fails to improve the AUPRC for dataset pbmc-ch, even if the hyperparameters are optimized specifically for pbmc-related datasets (Supplementary Figure S2). In contrast, optimal hyperparameters consistently improve AUPRC for the other five pbmc-related datasets, and the improvements are greater with specifically tuned hyperparameters (Figure 1 and Supplementary Figure S2). Such discrepancy is potentially due to the different doublet annotation techniques (cell hashing vs. demuxlet) and batch effects among those datasets. Further investigations, especially from the experimental perspective, are needed to reveal the impacts of these two factors on doublet detection.

Third, the optimal hyperparameters vary depending on the biological conditions and optimization objectives. There are no universal hyperparameters adaptive to all scenarios. The significant hyperparameters when optimizing AUPRC across all 16 datasets are *pc* and *nf*, with optimal values as 19 and 1252, respectively (Supplementary Table S2). If optimized on pbmc-related datasets, *nf* is no longer significant, and the optimal value of *pc* changes to 18. If optimized on HMEC-related datasets, *pc* is no longer significant, and the optimal value of *nf* changes to 1520. Depth is the only significant hyperparameter when optimizing the true positive and negative rate on all 16 datasets, with optimal values as 5 in both cases. This result indicates that existing and future doublet-detection methods need to fine-tune hyperparameters for a variety of biological conditions and accuracy measurements.

In summary, doublet detection is one essential step in the quality control of scRNA-seq data analysis. The hyperparameter configuration significantly impacts the performance of computational doublet-detection methods. Our study is the first attempt to systematically explore the optimal hyperparameters under various biological conditions and optimization objectives. Our study provides much-needed guidance for hyperparameter tuning in computational doublet-

detection methods. Future directions of our study include increasing the exploratory space by utilizing advanced experimental design strategies, e.g., space-filling design <sup>29,30</sup> and fractional factorial design <sup>31,32</sup>. Another direction is to optimize hyperparameters for other doublet-detection methods by our tuning strategy. More scRNA-seq datasets with experimentally annotated doublets could also be incorporated into the tuning process to enhance the generalizability of optimal hyperparameters.

## **Data Availability**

The 16 scRNA-seq datasets used in this study are available at Zenodo repository

<https://doi.org/10.5281/zenodo.4562782>

## References

1. Kolodziejczyk, A. A., Kim, J. K., Svensson, V., Marioni, J. C. & Teichmann, S. A. The technology and biology of single-cell RNA sequencing. *Mol. Cell* **58**, 610–620 (2015).
2. Saliba, A.-E., Westermann, A. J., Gorski, S. A. & Vogel, J. Single-cell RNA-seq: advances and future challenges. *Nucleic Acids Research* vol. 42 8845–8860 Preprint at <https://doi.org/10.1093/nar/gku555> (2014).
3. Wiedmeier, J. E., Noel, P., Lin, W., Von Hoff, D. D. & Han, H. Single-Cell Sequencing in Precision Medicine. *Cancer Treat. Res.* **178**, 237–252 (2019).
4. Aissa, A. F. *et al.* Single-cell transcriptional changes associated with drug tolerance and response to combination therapies in cancer. *Nat. Commun.* **12**, 1–25 (2021).
5. Sun, G. *et al.* Single-cell RNA sequencing in cancer: Applications, advances, and emerging challenges. *Molecular Therapy - Oncolytics* **21**, 183–206 (2021).
6. Noé, A., Cargill, T. N., Nielsen, C. M., Russell, A. J. C. & Barnes, E. The Application of Single-Cell RNA Sequencing in Vaccinology. *J Immunol Res* **2020**, 8624963 (2020).
7. Wolock, S. L., Lopez, R. & Klein, A. M. Scrublet: Computational Identification of Cell Doublets in Single-Cell Transcriptomic Data. *Cell Syst* **8**, 281-291.e9 (2019).
8. McGinnis, C. S., Murrow, L. M. & Gartner, Z. J. DoubletFinder: Doublet Detection in Single-Cell RNA Sequencing Data Using Artificial Nearest Neighbors. *Cell Syst* **8**, 329-337.e4 (2019).
9. Germain, P.-L., Lun, A., Garcia Meixide, C., Macnair, W. & Robinson, M. D. Doublet identification in single-cell sequencing data using scDblFinder. *F1000Res.* **10**, 979 (2021).
10. Bais, A. S. & Kostka, D. scds: computational annotation of doublets in single-cell RNA sequencing data. *Bioinformatics* Preprint at <https://doi.org/10.1093/bioinformatics/btz698> (2019).
11. Bernstein, N. J. *et al.* Solo: Doublet Identification in Single-Cell RNA-Seq via Semi-Supervised Deep Learning. *Cell Syst* **11**, 95-101.e5 (2020).

12. Xi, N. M. & Li, J. J. Benchmarking Computational Doublet-Detection Methods for Single-Cell RNA Sequencing Data. *Cell Systems* **12**, 176-194.e6 (2021).
13. Redko, I., Morvant, E., Habrard, A., Sebban, M. & Bennani, Y. *Advances in Domain Adaptation Theory*. (Elsevier, 2019).
14. Xi, N. M. & Li, J. J. Protocol for executing and benchmarking eight computational doublet-detection methods in single-cell RNA sequencing data analysis. *STAR Protocols* **2**, 100699 (2021).
15. Steinberg, D. M. & Hunter, W. G. Experimental Design: Review and Comment. *Technometrics* **26**, 71–97 (1984).
16. Hao, Y. *et al.* Integrated analysis of multimodal single-cell data. *Cell* **184**, 3573-3587.e29 (2021).
17. Chen, T. & Guestrin, C. XGBoost: A Scalable Tree Boosting System. in *Proceedings of the 22nd ACM SIGKDD International Conference on Knowledge Discovery and Data Mining* 785–794 (Association for Computing Machinery, 2016).
18. Box, G. E. P. & Draper, N. R. Empirical model-building and response surfaces. *Wiley series in probability and mathematical statistics*. **669**, (1987).
19. Box, G. E. P. & Wilson, K. B. On the Experimental Attainment of Optimum Conditions. *J. R. Stat. Soc. Series B Stat. Methodol.* **13**, 1–45 (1951).
20. Breusch, T. & Pagan, A. A Simple Test for Heteroscedasticity and Random Coefficient Variation. *Econometrica* **47**, 1287–1294 (1979).
21. Luecken, M. D. & Theis, F. J. Current best practices in single-cell RNA-seq analysis: a tutorial. *Mol. Syst. Biol.* **15**, (2019).
22. Probst, P., Boulesteix, A. L. & Bischl, B. Tunability: Importance of hyperparameters of machine learning algorithms. *J. Mach. Learn. Res.* (2019).
23. Hu, Q. & Greene, C. S. Parameter tuning is a key part of dimensionality reduction via deep variational autoencoders for single cell RNA transcriptomics. *Pac. Symp. Biocomput.* **24**, 362–373 (2019).

24. Raimundo, F., Vallot, C. & Vert, J.-P. Tuning parameters of dimensionality reduction methods for single-cell RNA-seq analysis. *Genome Biol.* **21**, 212 (2020).
25. Alles, J. *et al.* Cell fixation and preservation for droplet-based single-cell transcriptomics. *BMC Biol.* **15**, (2017).
26. Stoeckius, M. *et al.* Cell Hashing with barcoded antibodies enables multiplexing and doublet detection for single cell genomics. *Genome Biol.* **19**, 224 (2018).
27. Kang, H. M. *et al.* Multiplexed droplet single-cell RNA-sequencing using natural genetic variation. *Nat. Biotechnol.* **36**, 89–94 (2018).
28. McGinnis, C. S. *et al.* MULTI-seq: sample multiplexing for single-cell RNA sequencing using lipid-tagged indices. *Nature Methods* vol. 16 619–626 Preprint at <https://doi.org/10.1038/s41592-019-0433-8> (2019).
29. Wang, L., Xiao, Q. & Xu, H. Optimal maximin -distance Latin hypercube designs based on good lattice point designs. *Ann. Stat.* (2018).
30. Wang, L., Sun, F., Lin, D. K. J. & Liu, M.-Q. CONSTRUCTION OF ORTHOGONAL SYMMETRIC LATIN HYPERCUBE DESIGNS. *Stat. Sin.* **28**, 1503–1520 (2018).
31. Wang, L., Xu, H. & Liu, M.-Q. Fractional factorial designs for Fourier-cosine models. *Metrika* (2022) doi:10.1007/s00184-022-00881-2.
32. Wang, L. & Xu, H. A class of multilevel nonregular designs for studying quantitative factors. *Stat. Sin.* (2022) doi:10.5705/ss.202020.0223.

## Figures

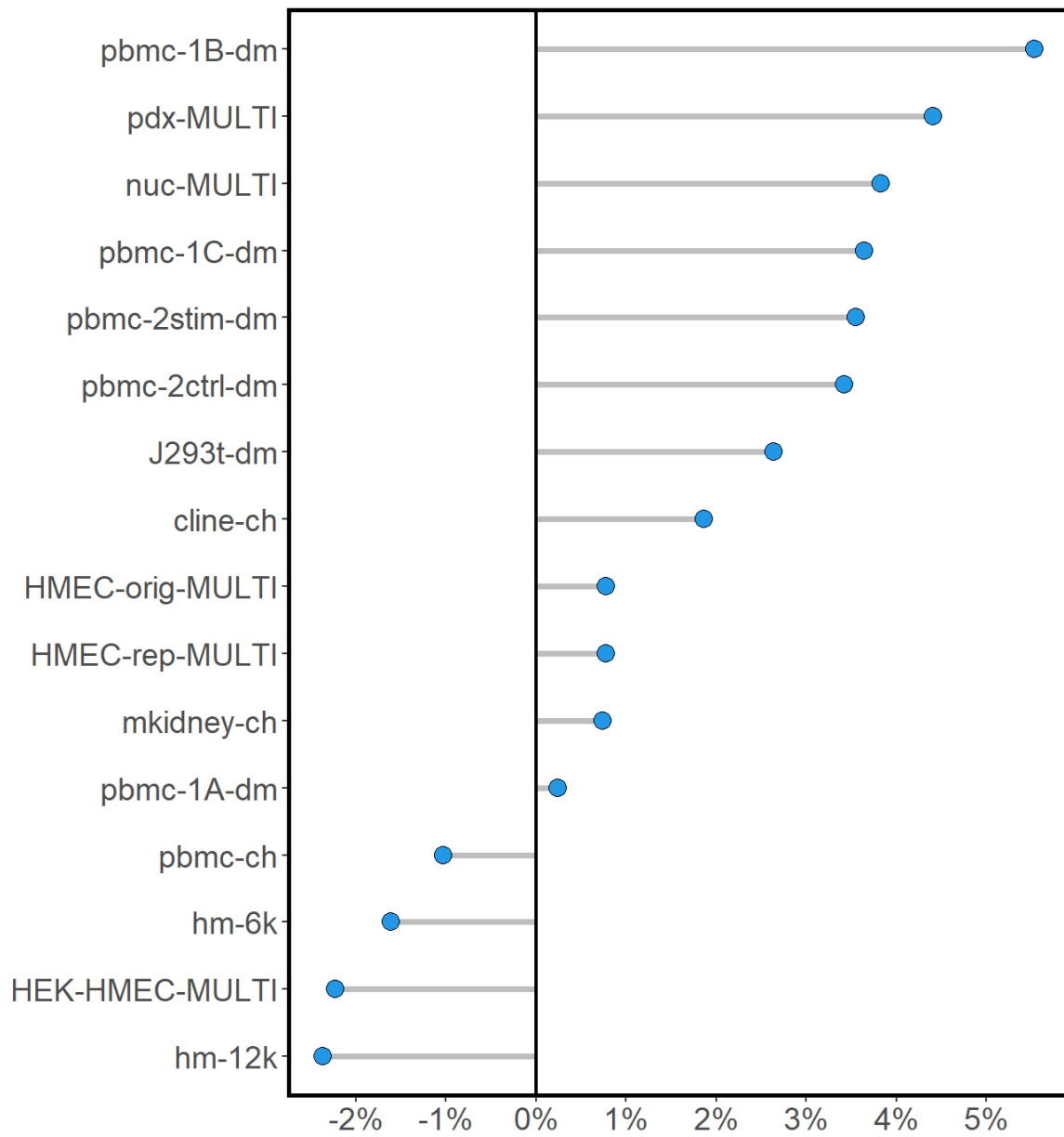


**Figure 1.** AUPRC improvement by hyperparameter optimization over the method's default settings on 16 scRNA-seq datasets.



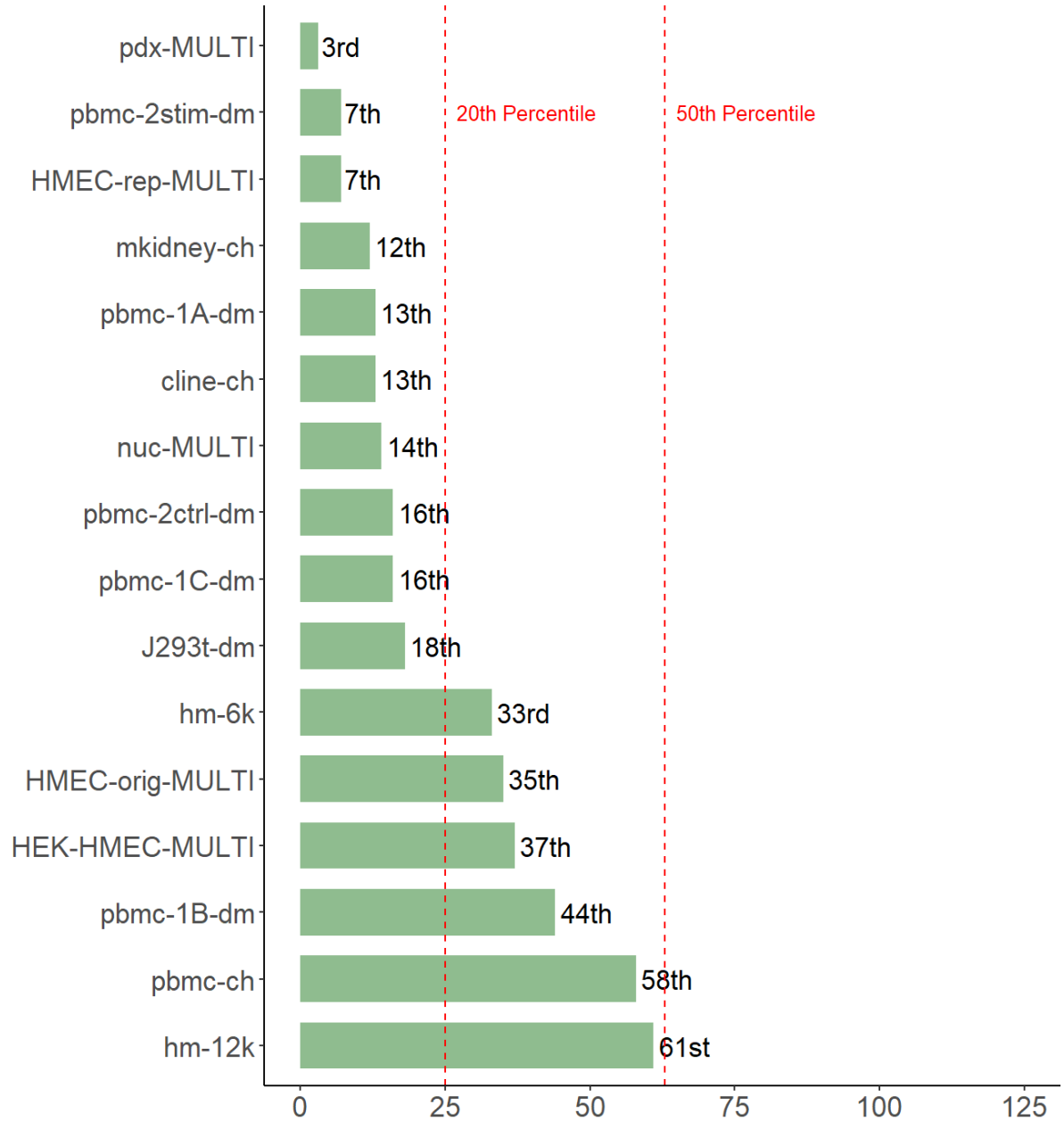


**Figure 2.** Rankings of optimal hyperparameter performances by AUPRC among 125 hyperparameter combinations on 16 datasets.

## Tables

**Table 1.** The 16 scRNA-seq datasets with experimentally annotated doublets in this study.

Dataset	Cell type	Droplet #	Gene #	Doublet rate	Doublet annotation technique
pbmc-ch	pbmc	15272	21639	16.66%	Cell hashing <sup>26</sup>
cline-ch	HEK293T, K562, KG1, THP1	7954	25221	18.42%	Cell hashing
mkidney-ch	mouse kidney	21179	18940	37.31%	Cell hashing
hm-12k	HEK293T, NIH3T3	12820	15106	5.69%	Species mixture <sup>25</sup>
hm-6k	HEK293T, NIH3T3	6806	15080	2.51%	Species mixture
pbmc-1A-dm	pbmc	3298	15170	3.64%	Demuxlet <sup>27</sup>
pbmc-1B-dm	pbmc	3790	15143	3.43%	Demuxlet
pbmc-1C-dm	pbmc	5270	15865	6.00%	Demuxlet
pbmc-2ctrl-dm	pbmc	13913	17584	11.49%	Demuxlet
pbmc-2stim-dm	pbmc	13916	17315	11.72%	Demuxlet
J293t-dm	jurkat, HEK293T	500	16374	8.40%	Demuxlet
pdx-MULTI	human breast cancer, mouse immune	10296	14025	12.79%	MULTI-seq <sup>28</sup>
HMEC-orig-MULTI	HMEC	26426	24199	13.50%	MULTI-seq
HMEC-rep-MULTI	HMEC	10580	17473	31.02%	MULTI-seq
HEK-HMEC-MULTI	HEK293T, HMEC	10641	23982	4.60%	MULTI-seq
nuc-MULTI	nuclei (HEK293T, MEF, Jurkat)	5578	21490	8.52%	MULTI-seq

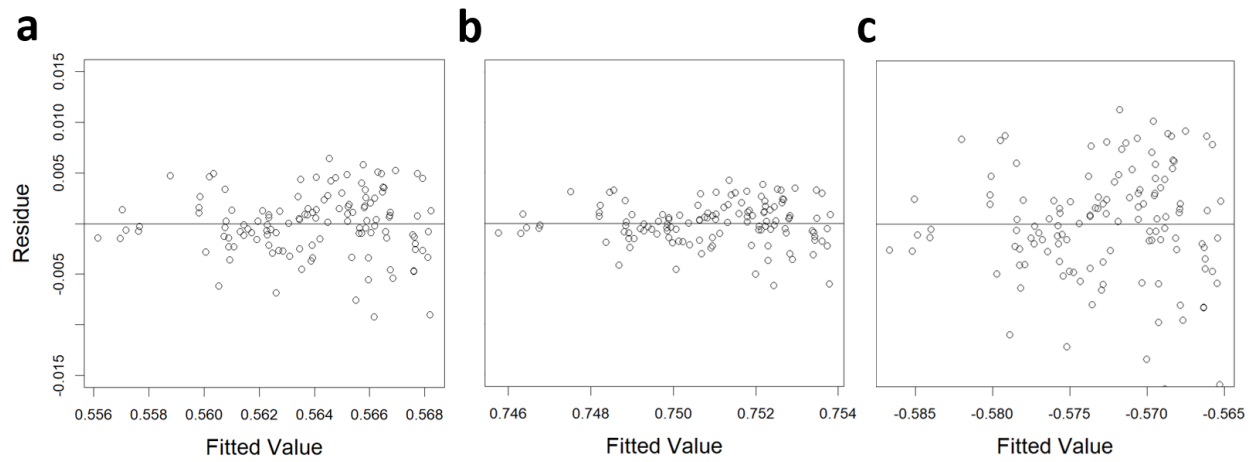
**Table 2.** The three hyperparameters and their default and exploratory values in this study.

<b>Hyperparameter</b>	<b>Default values</b>	<b>Exploratory values</b>
<i>nf</i>	1000	500, 1000, 1500, 2000, 2500
<i>pc</i>	10	5, 10, 15, 20, 25
<i>depth</i>	4	2, 3, 4, 5, 6

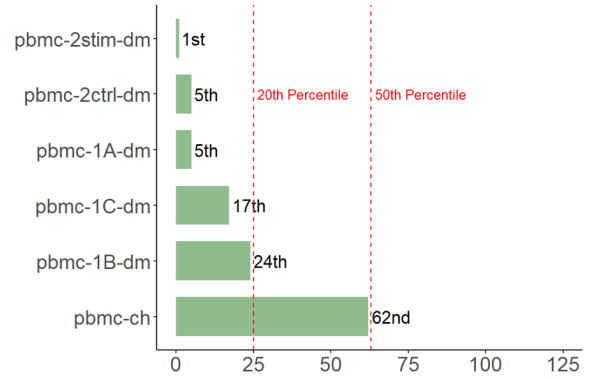
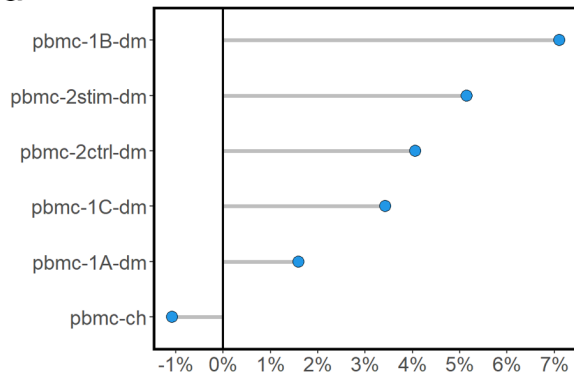
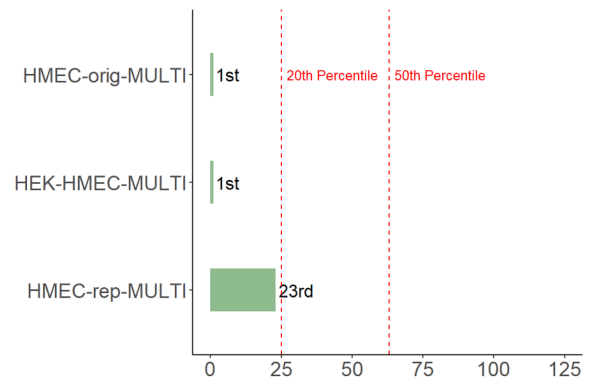
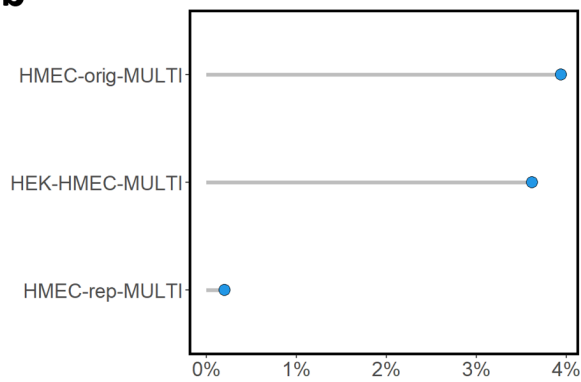
**Table 3.** The AUPRC of doublet detection under optimal and default hyperparameters. The last column shows the highest AUPRC achieved by one of the 125 hyperparameter combinations. The highest AUPRC between the optimum and default of each dataset is underscored.

<b>Dataset</b>	<b>Optimum</b>	<b>Default</b>	<b>Maximum</b>
cline-ch	<u>0.4280</u>	0.4202	0.4369
HEK-HMEC-MULTI	0.4723	0.4830	0.4966
HEK-orig-MULTI	<u>0.4911</u>	0.4873	0.5054
hm-12k	0.9281	0.9506	0.9850
hm-6k	0.9737	0.9896	0.9972
HMEC-rep-MULTI	<u>0.6010</u>	0.5964	0.6020
J293t-dm	<u>0.2052</u>	0.1999	0.2525
mkidney-ch	<u>0.6125</u>	0.6080	0.6183
nuc-MULTI	<u>0.4600</u>	0.4430	0.4704
pbmc-1A-dm	<u>0.5454</u>	0.5441	0.5693
pbmc-1B-dm	<u>0.4375</u>	0.4145	0.4818
pbmc-1C-dm	<u>0.5953</u>	0.5744	0.6082
pbmc-2ctrl-dm	<u>0.6980</u>	0.6749	0.7088
pbmc-2stim-dm	<u>0.7003</u>	0.6763	0.7124
pbmc-ch	0.6405	0.6472	0.6520
pdx-MULTI	<u>0.4457</u>	0.4268	0.4477

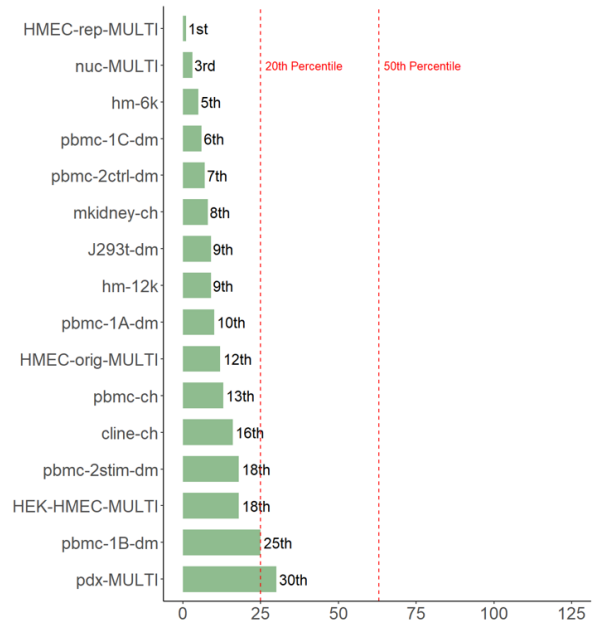
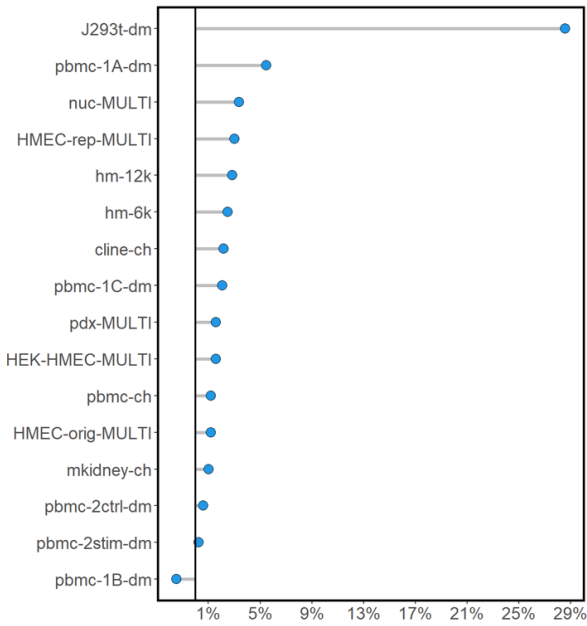
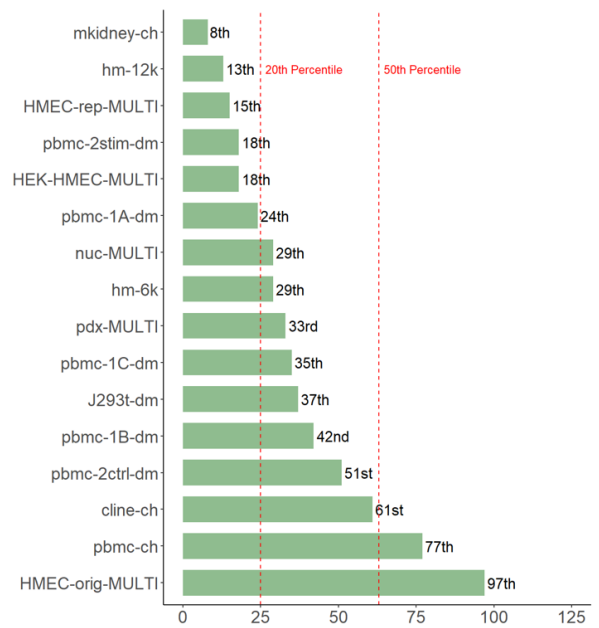
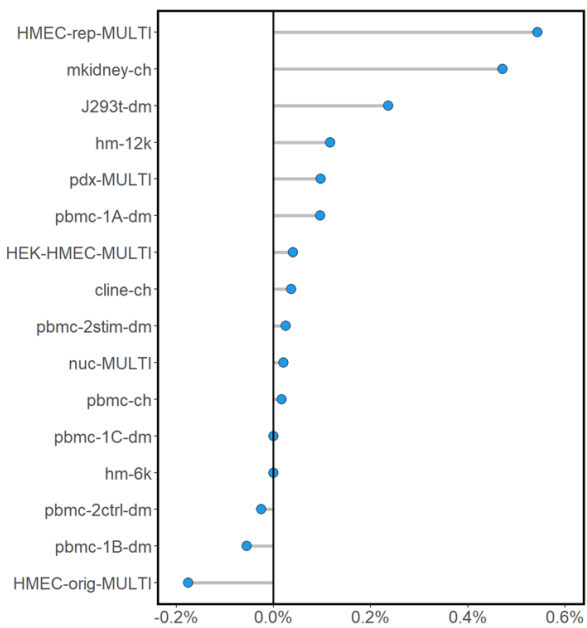
## Supplementary Figures



**Supplementary Figure S1.** Residue plots of model (1) on datasets before and after transformation on the response variable. All three figures have the same residue scale. **a**, No transformation. **b**, Square-root-transformation on response variable AUPRC. **c**, Natural-log-transformation on response variable AURPC.

**a****b**

**Supplementary Figure S2.** AUPRC improvement and ranking with hyperparameters optimized on datasets of different biological conditions. **a**, Optimized on pbmc-related datasets. **b**, Optimized on HMEC-related datasets.

**a****b**

**Supplementary Figure S3.** Double-detection improvement and ranking in terms of different measurements. **a**, Measured by true positive rate. **b**, Measured by true negative rate. The hyperparameters are optimized on all 16 scRNA-seq datasets

## Supplementary Tables

**Supplementary Table S1.** The significant hyperparameters and their raw optimal values before and after transformation on response variable AUPRC.

<b>Transformation</b>	<b>Significant hyperparameter</b>	<b>Optimal value</b>
No transformation	<i>nf, pc</i>	nf = 1351.661, pc = 19.181
Square root	<i>nf, pc</i>	nf = 1352.087, pc = 19.189
Natural log	<i>nf, pc</i>	nf = 1352.509, pc = 19.196



**Supplementary Table S2.** The significant hyperparameters in model (1) and their optimal values (rounding to the nearest integers) optimized on different biological conditions and accuracy metrics of doublet detection.

<b>Optimization subset</b>	<b>Optimization metric</b>	<b>Significant hyperparameter</b>	<b>Optimal value</b>
All	AUPRC	$pc, nf$	$pc = 19,$ $nf = 1352$
pbmc-related	AUPRC	$pc$	$pc = 18$
HMEC-related	AUPRC	$nf$	$nf = 1520$
All	True positive rate	$depth$	$depth = 5$
All	True negative rate	$depth$	$depth = 5$

**Supplementary Table S3.** The AUPRC of doublet detection under optimal and default hyperparameters on pbmc-related datasets. The last column shows the highest AUPRC achieved by one of the 125 hyperparameter combinations. The highest AUPRC between the optimum and default of each dataset is underscored.

<b>Dataset</b>	<b>Optimum</b>	<b>Default</b>	<b>Maximum</b>
pbmc-1A-dm	<u>0.5528</u>	0.5441	0.5693
pbmc-1B-dm	<u>0.4440</u>	0.4145	0.4818
pbmc-1C-dm	<u>0.5941</u>	0.5744	0.6082
pbmc-2ctrl-dm	<u>0.7023</u>	0.6749	0.7088
pbmc-2stim-dm	<u>0.7111</u>	0.6763	0.7124
pbmc-ch	0.6402	<u>0.6472</u>	0.6520

**Supplementary Table S4.** The AUPRC of doublet detection under optimal and default hyperparameters on HMEC-related datasets. The last column shows the highest AUPRC achieved by one of the 125 hyperparameter combinations. The highest AUPRC between the optimum and default of each dataset is underscored.

<b>Dataset</b>	<b>Optimum</b>	<b>Default</b>	<b>Maximum</b>
HEK-HMEC-MULTI	<u>0.5005</u>	0.4830	0.4966
HEK-orig-MULTI	<u>0.5065</u>	0.4873	0.5054
HMEC-rep-MULTI	<u>0.5976</u>	0.5964	0.6020

**Supplementary Table S5.** The true positive rate of doublet detection under optimal and default hyperparameters. The last column shows the highest true positive rate achieved by one of the 125 hyperparameter combinations. The larger true positive rate between optimum and default in each dataset is underscored.

<b>Dataset</b>	<b>Optimum</b>	<b>Default</b>	<b>Maximum</b>
cline-ch	<u>0.3543</u>	0.3468	0.3604
HEK-HMEC-MULTI	<u>0.5297</u>	0.5215	0.5358
HEK-orig-MULTI	<u>0.8973</u>	0.8726	0.9233
hm-12k	<u>0.9591</u>	0.9357	0.9649
hm-6k	<u>0.5028</u>	0.4969	0.5121
HMEC-rep-MULTI	<u>0.5314</u>	0.5158	0.5314
J293t-dm	<u>0.2143</u>	0.1667	0.2381
mkidney-ch	<u>0.5875</u>	0.5816	0.5894
nuc-MULTI	<u>0.4505</u>	0.4358	0.4505
pbmc-1A-dm	<u>0.6417</u>	0.6083	0.6500
pbmc-1B-dm	0.5154	<u>0.5231</u>	0.5462
pbmc-1C-dm	<u>0.6266</u>	0.6139	0.6266
pbmc-2ctrl-dm	<u>0.7196</u>	0.7153	0.7240
pbmc-2stim-dm	<u>0.7192</u>	0.7174	0.7253
pbmc-ch	<u>0.6346</u>	0.6271	0.6369
pdx-MULTI	<u>0.4374</u>	0.4305	0.4487

**Supplementary Table S6.** The true negative rate of doublet detection under optimal and default hyperparameters. The last column shows the highest true negative rate achieved by one of the 125 hyperparameter combinations. The larger true negative rate between optimum and default in each dataset is underscored.

<b>Dataset</b>	<b>Optimum</b>	<b>Default</b>	<b>Maximum</b>
cline-ch	<u>0.8530</u>	0.8527	0.8558
HEK-HMEC-MULTI	<u>0.9774</u>	0.9770	0.9777
HEK-orig-MULTI	<u>0.9936</u>	0.9925	0.9955
hm-12k	<u>0.9986</u>	0.9986	0.9994
hm-6k	0.9199	<u>0.9216</u>	0.9239
HMEC-rep-MULTI	<u>0.7868</u>	0.7825	0.7895
J293t-dm	<u>0.9279</u>	0.9258	0.9323
mkidney-ch	<u>0.7546</u>	0.7511	0.7558
nuc-MULTI	<u>0.9479</u>	0.9477	0.9490
pbmc-1A-dm	<u>0.9865</u>	0.9855	0.9871
pbmc-1B-dm	0.9831	<u>0.9836</u>	0.9844
pbmc-1C-dm	<u>0.9756</u>	0.9756	0.9764
pbmc-2ctrl-dm	0.9629	<u>0.9631</u>	0.9643
pbmc-2stim-dm	<u>0.9629</u>	0.9626	0.9637
pbmc-ch	<u>0.9257</u>	0.9256	0.9276
pdx-MULTI	<u>0.9176</u>	0.9167	0.9194